PHYSICAL REVIEW B 73, 184424 (2006)

Berezinskiĭ–Kosterlitz–Thouless transition in two–dimensional lattice gas models

Hassan CHAMATI* and Silvano ROMANO†
Unitá CNISM e Dipartimento di Fisica "A. Volta", Università di Pavia, via A. Bassi 6, I-27100 Pavia, ITALY

We have considered two classical lattice–gas models, consisting of particles that carry multicomponent magnetic momenta, and associated with a two–dimensional square lattices; each site can host one particle at most, thus implicitly allowing for hard–core repulsion; the pair interaction, restricted to nearest neighbors, is ferromagnetic and involves only two components. The case of zero chemical potential has been investigated by Grand–Canonical Monte Carlo simulations; the fluctuating occupation numbers now give rise to additional fluid–like observables in comparison with the usual saturated–lattice situation; these were investigated and their possible influence on the critical behaviour was discussed. Our results show that the present model supports a Berezinskiĭ–Kosterlitz–Thouless phase transition with a transition temperature lower than that of the saturated lattice counterpart due to the presence of "vacancies"; comparisons were also made with similar models studied in the literature.

PACS numbers: 75.10.Hk, 05.50.+q, 64.60.–i
Keywords: lattice gases, classical spin models, Berezinskiĭ–Kosterlitz–Thouless transition.

I. INTRODUCTION

Planar rotators are models with potential interactions involving two–component spins; on the other hand, in the XY model, the spins have three components, only two of which are involved in the interaction, and the XY model can be regarded as an extremely anisotropic (easy–plane) Heisenberg model. Actually, the terminological convention adopted here as well as by other Authors is not always followed, and the name "XY model" is sometimes used in the Literature to indicate planar rotators; on the other hand, both models are known to produce the same universality class. The two named models have been extensively studied, and possess a rich variety of applications in Statistical as well as Condensed Matter Physics[1,2,3].

These models have been especially studied in their saturated-lattice (SL) version, where each site is occupied by a particle; as for symbols, classical SL spin models are first defined here: we consider a classical system, consisting of $n-$component unit vectors $\mathbf{u}_k$ (usually $n = 2, 3$), associated with a $d-$dimensional (bipartite) lattice $\mathbb{Z}^d$ (mostly $d = 2$); let $\mathbf{x}_k$ denote dimensionless coordinates of the lattice sites, and let $u_{k,\alpha}$ denote Cartesian spin components with respect to an orthonormal basis $\mathbf{e}_\alpha$; particle orientations are parameterized by usual polar angles $\{\varphi_j\}$ ($n = 2$) or spherical ones $\{(\theta_j, \phi_j)\}$ ($n = 3$);

The interaction potentials considered here are assumed to be translationally invariant, restricted to nearest–neighbours, ferromagnetic (FM); they are, in general, anisotropic in spin space, and possess $O(2)$ symmetry at least:

$$\Psi_{jk} = -\epsilon\Omega_{jk}, \tag{1}$$

where

$$\Omega_{jk} = a u_{j,n}u_{k,n} + b\sum_{\alpha<n} u_{j,\alpha}u_{k,\alpha}; \qquad \epsilon > 0,\ 0 \le a \le b,\ b > 0,\ \max(a,b) = 1. \tag{2}$$

Here ϵ is a positive quantity setting energy and temperature scales (i.e. $T = k_B t/\epsilon$, where t denotes the absolute temperature); the corresponding (scaled) Hamiltonian reads

$$\Lambda = -\sum_{\{j<k\}} \Omega_{jk}, \tag{3}$$

where $\sum_{\{j<k\}}$ is restricted to nearest neighbours, with each distinct pair being counted once. When $d = 1, 2$, potential models defined by Eq. (2) produce orientational disorder at all finite temperatures (thus no orientational ordering transition at finite temperature)[4,5]; in the following, the discussion shall be essentially restricted to the two cases $n = 2,\ a = b = 1$ (PR) and $n = 3,\ a = 0,\ b = 1$ (XY), respectively.

It is by now well known that the PR model defined by $d = 2$ supports a transition to a low–temperature phase with slow (inverse–power–law) decay of the correlation function and infinite susceptibility; this is the very extensively studied Berezinskiĭ–Kosterlitz–Thouless (BKT) transition (see, e.g. Refs.[1,2,3,6,7,8] and others quoted therein), whose existence was proven rigorously by Fröhlich and Spencer[6]: the transition temperature was estimated to be $\Theta_{PR} = 0.88 \pm 0.01$[7], and a more recent and more refined result is $\Theta_{PR} = 0.8929$[8]; the specific heat exhibits a maximum at a higher temperature[7,9]. Moreover, anisotropic models defined by $d = 2,\ n = 3,\ 0 \le a < b$ have been studied as well and proven to support a BKT transition when the ratio a/b is sufficiently small[10]; an estimate of the transition temperature for the XY case is given by $\Theta_{XY} = 0.700 \pm 0.005$[11,12,13].

Lattice–gas (LG) extensions of the SL models can be defined as well, where each lattice site hosts one particle at most, and site occupation is also controlled by the chemical potential μ; such models have often been used in connection with alloys and absorption; this methodology somehow allows for pressure and density effects. Lattice–gas (LG) extensions of the continuous–spin potential model considered here are defined by Hamiltonians

$$\Lambda = \sum_{\{j<k\}} \nu_j\nu_k(\lambda - \Omega_{jk}) - \mu N, \qquad N = \sum_k \nu_k, \tag{4}$$

where $\nu_k = 0, 1$ denotes occupation numbers; notice that $\lambda \leq 0$ reinforces the orientation–dependent term, whereas $\lambda > 0$ opposes it, and that a finite value of λ only becomes immaterial in the SL limit $\mu \to +\infty$.

For a square lattice, the SL–PR model produces a low–temperature BKT transition; the existence of such a transition for the LG counterpart has been proven rigorously as well[14]. In addition to the named rigorous results, still comparatively little is known about the above magnetic LG models with continuous spins, in marked contrast to the vast amount of information available for their SL counterparts; for example, as far as we could check in the Literature, their simulation study only started at the end of the 1990's[15,16].

A few years before the existence of a BKT transition was proven for the LG–PR model[14], the same model had been investigated by Monte Carlo simulation in the Grand–Canonical ensemble, and in the absence of a purely positional interaction, i.e. $\lambda = 0$[15]. Simulations were carried out for $\mu = 0.1$ and $\mu = -0.2$, and showed that the BKT transition survives, even for mildly negative μ, and that the transition temperature is an increasing function of μ, in broad qualitative agreement with previous Renormalization Group (RG) studies[17,18,19].

The Hamiltonian (Eq. (4)) can be interpreted as describing a two–component system consisting of interconverting "real" ($\nu_k = 1$) and "ghost", "virtual" or ideal–gas particles ($\nu_k = 0$); both kinds of particles have the same kinetic energy, μ denotes the excess chemical potential of "real" particles over "ideal" ones, and the total number of particles equals the number of available lattice sites (semi–Grand–Canonical interpretation). The semi–Grand–Canonical interpretation was also used in early studies of the two–dimensional planar rotator, carried out by the Migdal–Kadanoff RG techniques, and aiming at two–dimensional mixtures (films) of ^{3}He and ^{4}He[17,18,19], where non–magnetic impurities correspond to ^{3}He. In addition to phase separations, the results in Refs.[17,18,19] show that, in a régime of low fraction of non–magnetic impurities, the paramagnetic phase undergoes a BKT transition.

Notice also that the above Hamiltonian (Eq. (4)) describes a situation of *annealed* dilution; on the other hand, models in the presence of *quenched* dilution, and hence the effect of disorder on the BKT transition, have been investigated using the PR model[20,21,22,23,24,25] and very recently the XY model[25]; it was found that a sufficiently weak disorder does not destroy the transition, which survives up to a concentration of vacancies close to the percolation threshold.

In this paper, we present an extensive study of the ferromagnetic LG–PR and LG–XY models, whose Hamiltonian can be explicitly written as

$$\Lambda = \sum_{\{j<k\}} \nu_j \nu_k \left[\lambda - (u_{j,1} u_{k,1} + u_{j,2} u_{k,2}) \right] - \mu N, \qquad (5)$$

in order to gain insights into their critical behaviour. The models are further simplified by choosing $\lambda = 0$, i.e. no pure positional interactions; Let us also remark that two–component spins are involved in the PR case, whereas XY involves three–component spins but only two of their components are involved in the interaction: in this sense the two models entail different anchorings with respect to the horizontal plane in spin space; moreover, an even greater variety of anchorings can be realized via the recently introduced generalized XY models[26,27].

The rest of the paper is organized as follows: in Section II we discuss details our simulation procedure. Section III is devoted to the discussion of simulation results: we have found evidence pointing to a BKT transition, and used the relevant finite–size scaling theory to locate it. Possible effects of the chemical potential on the nature of the transition are discussed in Section IV, which summarizes our results.

II. MONTE CARLO SIMULATIONS

A detailed treatment of Grand–Canonical simulations can be found in or via Refs.[15,28,29]; the method outlined here has already been used in our previous studies of other LG models[16,28,30]. To avoid surface effects simulations were carried out on periodically repeated samples, consisting of $V = L^2$ sites, $L = 40, 80, 120, 160$; calculations were carried out in cascade, in order of increasing reduced temperature T.

The two basic MC steps used here were Canonical and semi–Grand–Canonical attempts; in addition two other features were implemented[31,32]: (i) when a lattice sites was visited, Canonical or semi–Grand–Canonical steps were randomly chosen with probabilities $\mathcal{P}_{\rm can}$ and $\mathcal{P}_{\rm GC}$, respectively; we used $\mathcal{P}_{\rm can}/\mathcal{P}_{\rm GC} = n - 1$, since spin orientation is defined by $(n-1)$ angles, versus one occupation number and (ii) sublattice sweeps (checkerboard decomposition)[31,32]; thus each sweep (or cycle) consisted of $2V$ attempts, first V attempts where the lattice sites was chosen randomly, then $V/2$ attempts on lattice sites of odd parity, and finally $V/2$ attempts on lattice sites on even parity. Equilibration runs took between 25 000 and 200 000 cycles, and production runs took between 250 000 and 1 000 000; macrostep averages for evaluating statistical errors were taken over 1 000 cycles. Different random–number generators were used, as discussed in Ref.[32].

Computed observables included mean Hamiltonian per site and its temperature derivative (specific heat at constant μ and V), density and its derivatives with respect to temperature and chemical potential, defined by

$$H^* = \frac{1}{V} \langle \Lambda \rangle , \qquad (6)$$

$$\rho = \frac{1}{V} \langle N \rangle , \qquad (7)$$

and by the fluctuation formulae (see e.g.[29])

$$\rho_T = \left. \frac{\partial \rho}{\partial T} \right|_{\mu,V} = \frac{1}{VT^2} \left[\langle N\Lambda \rangle - \langle N \rangle \langle \Lambda \rangle \right], \qquad (8)$$

$$\rho_\mu = \left. \frac{\partial \rho}{\partial \mu} \right|_{T,V} = \frac{1}{VT} \left[\left\langle N^2 \right\rangle - \langle N \rangle^2 \right], \qquad (9)$$

$$\frac{C_{\mu,V}}{k_B} = \frac{1}{k_B} \frac{1}{V} \left. \frac{\partial \langle \Lambda \rangle}{\partial T} \right|_{\mu,V} = \frac{1}{VT^2} \left[\left\langle \Lambda^2 \right\rangle - \langle \Lambda \rangle^2 \right]. \qquad (10)$$

We also calculated mean in–plane magnetic moment per site and in–plane susceptibility defined by

$$M = \frac{1}{V}\left\langle \sqrt{\mathbf{F}\cdot\mathbf{F}}\right\rangle \tag{11}$$

and

$$\chi = \frac{1}{VT}\left\langle \mathbf{F}\cdot\mathbf{F}\right\rangle, \tag{12}$$

where

$$\mathbf{F} = \sum_k \nu_k \left(u_{k,1}\mathbf{e}_1 + u_{k,2}\mathbf{e}_2\right), \tag{13}$$

taking into account only the in–plane components of the vector spin.

A square sample of V sites contains $2V$ distinct nearest–neighbouring pairs of lattice sites; we worked out pair occupation probabilities, i.e. the mean fractions R_{JK} of pairs being both empty ($R_{ee} = \left\langle (1-\nu_j)(1-\nu_k)\right\rangle$), both occupied ($R_{oo} = \left\langle \nu_j\nu_k\right\rangle$), or consisting of an empty and an occupied site ($R_{eo} = \left\langle (1-\nu_j)\nu_k + (1-\nu_k)\nu_j\right\rangle$). It should be noted that $R_{ee} + R_{oo} + R_{eo} = 1$.

Short– and long–range positional correlations, were compared by means of the excess quantities

$$R'_{oo} = \ln\left(\frac{R_{oo}}{\rho^2}\right),\ R''_{oo} = R_{oo} - \rho^2, \tag{14}$$

collectively denoted by R^*_{oo} (notice that these two definitions entail comparable numerical values).

Quantities such as ρ, ρ_T, ρ_μ and the above pair correlations R_{JK} or R^*_{oo} can be defined as "fluid–like", in the sense that they all go over the trivial constants in the SL limit. Let us also remark that some of the above definitions (e.g. $C_{\mu,V}$ and ρ_T) involve the total potential energy both in the stochastic variable and in the probability measure ("explicit" dependence), whereas some other definitions, e.g. ρ_μ or the quantities R_{JK}, involve the total potential energy only in the probability measure ("implicit" dependence).

III. SIMULATION RESULTS

We start by discussing the outcome of the simulations performed for the LG–XY model. Results for a number of observables, such as the mean energy per site H^*, and density ρ (not reported here) were found to evolve with temperature in a smooth way, and to be independent of sample sizes; the derivatives $C_{\mu,V}$ and ρ_T (both plotted on FIG. 1) showed a rather smooth trend with temperature, and a "sharp" peak at $T \approx 0.6$, around which the sample–size dependence of results became *slightly* more pronounced; notice that neither the specific heat nor ρ_T are exhibiting a divergence as a function of the temperature.

At all investigated temperatures simulation results for M (not reported here) exhibited the expected power–law decay

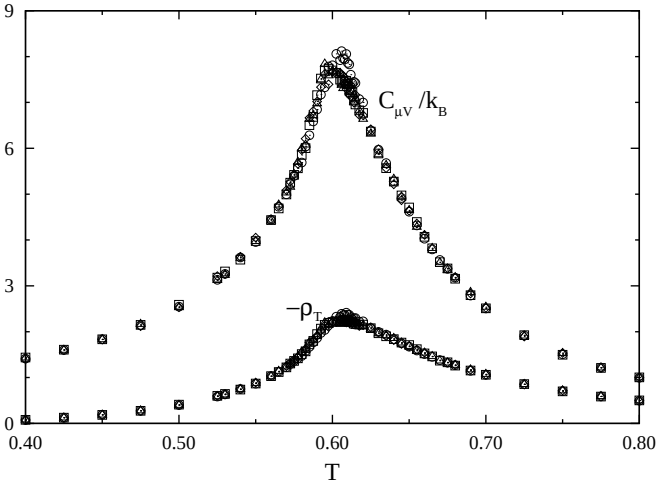

FIG. 1: Simulation estimates for the specific heat per site and for $-\rho_T$, obtained with different sample sizes: circles: $L = 40$; squares: $L = 80$; triangles: $L = 120$; diamonds: 160. The value $\mu = 0$ was used in the present calculations. Statistical errors for $C_{\mu,V}$, not reported, range between 1 and 3%; otherwise, here and in the following Figures, statistical errors fall within symbol sizes.

with increasing sample size, i.e. they were well fitted by the relation

$$\ln M = -b_1 \ln L + b_0, \qquad b_1 > 0, \tag{15}$$

where the ratio $b_1(T)/T$ was found to increase with temperature; a spin–wave analysis of the SL–PR (Refs.[33,34] and those quoted therein) predicts a similar sample–size dependence, in agreement with simulation results for the present model; furthermore, in the low–temperature limit b_1 becomes proportional to T.

The behaviours of specific heat and susceptibility (FIG. 2) suggest that the LG–XY model undergoes a BKT–like phase transition. According to the BKT theory, in the thermodynamic limit, the in–plane susceptibility, χ, diverges exponentially while approaching the transition temperature Θ in the high temperature region[2] i.e.

$$\chi \sim a_\chi \exp\left[b_\chi\,(T-\Theta)^{-\frac{1}{2}}\right]; \qquad T \to \Theta^+ \tag{16}$$

and remains infinite in the low temperature region $T < \Theta$.

For a finite sample with volume $V = L^2$, the situation is different, since the susceptibility obeys the constraint $\chi \le V/T$; thus χ is always finite, and its exponential divergence in the transition region is rounded, because of the important finite–size effects. Actually, results for $\ln\chi$ versus temperature (FIG. 2) were found to be independent of sample size when $T \gtrsim 0.62$, and showed a recognizable increase with it (a power–law dependence of χ on L) when $T \lesssim 0.6$.

In the critical region, i.e. $T \sim \Theta$, the correlation length is of the same order as the linear size, L, of the system. In this case, the exponential divergence disappears in the critical region, but a reminiscence of the divergence can still be found in the behaviour of χ at higher temperatures, where the correlation length is still small compared to large linear system

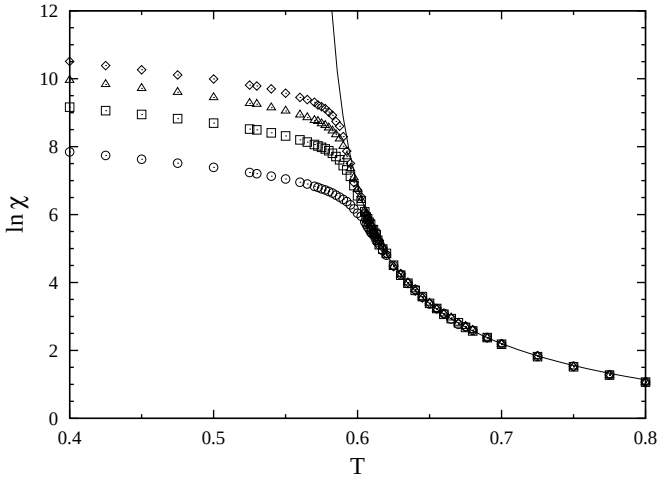

FIG. 2: Simulation estimates for the logarithm of the magnetic susceptibility χ versus temperature, obtained with different sample sizes; same meaning of symbols as in Fig. 1. The solid curve is obtained by fitting to equation (16) with data corresponding to $L = 160$.

sizes and finite–size effects can be neglected. We first fitted our MC results obtained for the largest sample size and for temperatures in the range $0.60 \lesssim T \lesssim 0.62$ to eq. (16), and obtained evidence of the exponential divergence of the susceptibility (see FIG. 2), and an estimated transition temperature $\Theta = 0.57 \pm 0.01$, with $a_\chi = 0.123 \pm 0.005$ and $b_\chi = 1.55 \pm 0.01$.

We checked our results by using data on a wider range of temperatures extending up to 0.70, and which yielded a consistent result. In the following we refine our results using a more elaborate method, namely the finite-size scaling theory. Details on this procedure can be found in or via reference[12].

In the temperature region where the singularity of χ is rounded the finite–size scaling theory holds, i.e. the correlation length ξ is proportional to the size of the sample, $\xi \sim L$. From the behaviour of the magnetic susceptibility $\chi \sim \xi^{2-\eta}$, with $\eta = 1/4$[2], we end up with

$$\chi(\Theta) \sim L^{2-\eta}, \tag{17}$$

where we have omitted the corrections arising from the presence of the background (analytic) contributions to the finite–size scaling.

The temperature region around $T = 0.57$, was analyzed in greater detail, at first by carrying out a linear fit of $\ln\chi$ versus $\ln L$ and extracting η from the slope; the values were found to be $\eta(T) = 0.223 \pm 0.008$, 0.244 ± 0.012, 0.255 ± 0.007, 0.273 ± 0.005, 0.308 ± 0.015 for $T = 0.5700, 0.5725, 0.5750, 0.5775, 0.5800$, respectively. A non–linear square fit, based on equation (17), was attempted as well, and yielded results consistent with these ones; it also proved convenient for result visualization to plot $\ln(\chi L^{-7/4})$ versus $\ln L$ (FIG. 3). Thus the transition temperature is estimated to be $\Theta = 0.574 \pm 0.003$, in agreement with the above mentioned result obtained by fitting the data of the susceptibility in the high temperature region; at this temperature we expect the value of η to be $\frac{1}{4}$ to within statistical errors. This result shows that the presence of "vacancies" in the sample reduce the transition temperature by approximately 18% compared to the SL transition temperature, but does not change its nature.

TABLE I: Comparison of the transition temperatures, Θ_{PR}, of the LG–PR model obtained in Ref.[15] and those obtained using the finite–size scaling presented in the present paper.

μ	Θ_{PR} (Ref.[15])	Θ_{PR} (present work)
−0.2	0.73 ± 0.01	0.71 ± 0.01
0.1	0.79 ± 0.01	0.75 ± 0.01

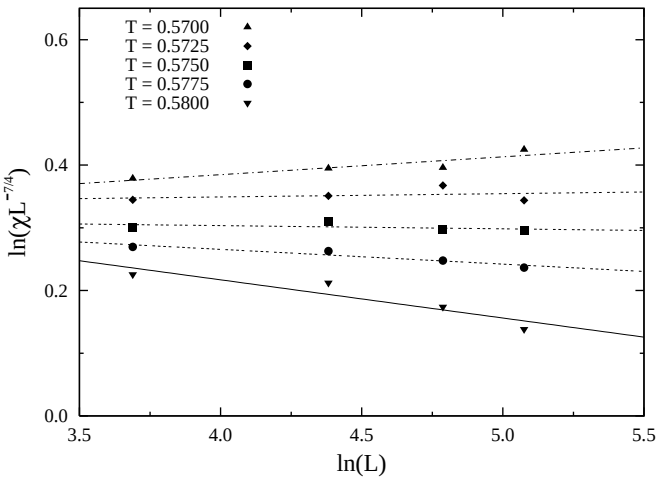

FIG. 3: Plot of $\ln\left(\chi L^{-7/4}\right)$ versus $\ln L$. Here the curve closest to a horizontal straight line signals the transition.

The PR counterpart of the present model had been investigated in Ref.[15], where a maximum sample size corresponding to $L = 80$ was used. Moreover, in that paper the transition temperature was estimated as the temperature where χ started exhibiting a power–law dependency on L. Calculations had been carried out with two different values of the chemical potential, $\mu = -0.2$ and $\mu = +0.1$, respectively (see e.g. Table I); the transition had been found to survive in both cases (even with a slightly negative value), and the transition temperature had been found to increase with increasing μ, in qualitative agreement with previous RG results[15].

For further comparison we reexamined the results obtained in the case of the LG–PR model in two ways. On the one hand, the above finite–size analysis was applied to the simulation data produced in Ref.[15]. The transition temperatures, reported in Table I, corresponding to the two values of the chemical potential used were found to be lower than the ones reported previously. The behaviour of the μ–dependence of the temperature was similar for both methods. On the other, in order to achieve a better comparison with the present case, simulations were run *anew* for the case $\mu = 0$, using same sample sizes as for the LG–XY counterpart ($L = 40, 80, 120, 160$). The thermodynamic quantities of interest were found to behave qualitatively in a similar fashion as those obtained in the framework of the XY model.

A detailed investigation of the susceptibility via the above finite–size scaling procedure resulted in a BKT–like transition

with a transition temperature estimate of 0.733 ± 0.003, corresponding to a particle density of 0.924 ± 0.003. The transition temperature in this case was found to be 18% lower than the case of the planar rotator SL counterpart.

As for other fluid–like quantities obtained within the framework of LG–XY, the plot of the derivative ρ_μ (FIG. 4) against the temperature exhibited a smooth evolution, a broad maximum at $T \approx 0.625$ and a comparatively weak sample–size dependence; pair occupation probabilities R_{JK} were found to be essentially independent of sample size, similarly to quantities such as H^* and ρ; their results for the largest sample size $L = 160$ are presented in FIG. 4 as well; the three quantities evolve with temperature in a gradual and monotonic way, and their plots suggest inflection points between $T = 0.6$ and $T = 0.625$, roughly corresponding to the maximum in ρ_μ. Short– and long–range positional correlations have been compared via the excess quantities R^*_{oo}, whose simulation results for the largest sample size are reported in FIG. 5, showing a broad maximum well above the transition temperature; notice also that R^*_{oo} remains rather small, reflecting the absence of a purely positional term in the interaction potential. In general it has been found that the obtained properties exhibit a recognizable similarity with with the counterparts for the isotropic LG–PR model[15]. Some other remarks are appropriate, concerning the temperature dependence of fluid–like properties; let us recall that our potential model contains no explicit positional interaction, i.e $\lambda = 0$ in Eq. (5), so that positional properties are essentially driven by the orientation-dependent pair potential. Similarities and differences in the above plots for $C_{\mu,V}$ and ρ_T on the one hand (FIG. 1), and ρ_μ or R_{JK} (FIG. 4) on the other hand, can then be correlated with the "implicit" or "explicit" dependencies of the named quantities on the potential energy (see remarks at the end of the previous section); the pair interaction energy changes most rapidly at $T \approx 0.6$, and this is reflected by narrow peaks in $C_{\mu,V}$ and ρ_T; conversely, quantities with "implicit dependence" on the pair interaction energy are less affected by the change, as shown by a broader peak at higher temperature $T \approx 0.625$.

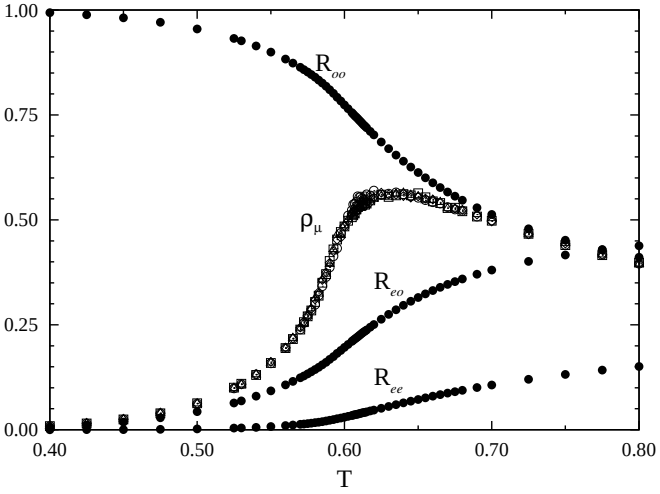

FIG. 4: Simulation estimates for the three pair occupation probabilities R_{JK} obtained for a two–dimensional sample with linear size $L = 160$, along with simulation estimates for ρ_μ, obtained with different sample sizes; same meaning of symbols as in FIG. 1.

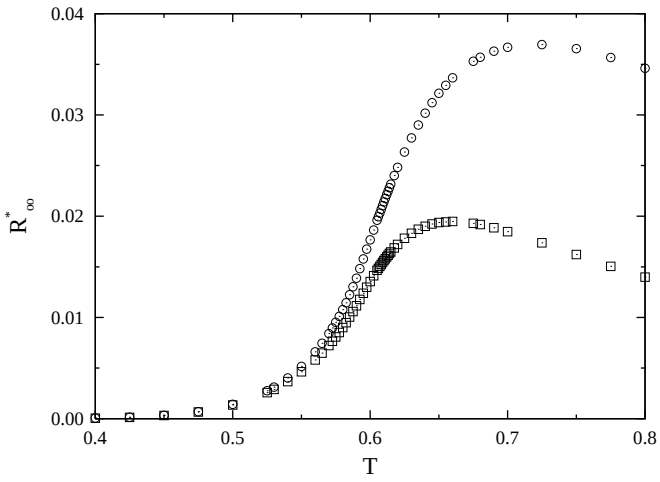

FIG. 5: Simulation estimates for the quantities R^*_{oo}; discrete symbols have been used for simulation results obtained with $L = 160$, and have the following meanings: circles: R'_{oo}; squares: R''_{oo}.

IV. CONCLUDING REMARKS

In this paper, we have investigated two magnetic lattice–gas models living on two–dimensional lattices, i.e. PR and XY, respectively. We have studied both lattice–gas models, in the absence of a pure positional interaction, using semi–Grand–Canonical Monte Carlo Simulation. In the case of zero chemical potential a number of thermodynamic quantities observable, including some characteristic of fluid systems, were computed. In general it has been found that the obtained properties for both models exhibit a recognizable qualitative similarity.

Results for the susceptibility yield consistent evidence of the existence of a BKT transition, suggesting the estimates $\Theta_{XY} = 0.574 \pm 0.003$ and $\Theta_{PR} = 0.733 \pm 0.003$ for the transition temperatures, with corresponding densities at transition $\rho_{XY} = 0.918 \pm 0.004$ and $\rho_{PR} = 0.924 \pm 0.003$, respectively. These results are consistent with those reported in Ref.[25] obtained in the framework of models describing quenched dilution; the ratio of the transition temperatures of the LG models to the SL ones is approximately 0.82. The peak of the specific heat falls closer to Θ_{BKT} than for the SL counterpart; this can be interpreted as reflecting the fact that, since $\lambda = 0$, the strengthening of short–range orientational correlations also brings about a more rapid increase of density, and hence, in turn, of H^*.

As for the possible μ–dependence of the present results, let us first notice that, since $(\partial\rho/\partial\mu)_{T,V} > 0$, it is reasonable to expect that χ, and hence Θ_{LG}, are increasing functions of μ. On the other hand, the ground–state energy for the SL counterpart is $-V_0$ per site, where $V_0 = 2$; thus the lattice is essentially saturated when $T \leq 1$ and μ exceeds a few multiples of V_0 (say μ ranging between 5 and $10V_0$); at the other ex-

treme, when μ is negative and of comparable magnitude, one expects an essentially empty lattice, where no BKTLT should survive. Moreover, a BKTLT may still survive if μ is negative but not too large in magnitude; this conjecture is supported by RG studies for the LG–PR[17,18,19], and was confirmed by the simulation results obtained in Ref.[15]; it also agrees with the conclusions of references[22,23,24,25] for two–dimensional magnets with quenched dilution; for large negative μ, the named RG treatments predict phase separation, i.e. a first–order transition between a BKT and a paramagnetic phase, and eventually the disappearance of the BKT phase. We expect to investigate the μ–dependence of the transition temperature in a more detailed way in future work.

Acknowledgements

The present extensive calculations were carried out, on, among other machines, workstations, belonging to the Sezione di Pavia of Istituto Nazionale di Fisica Nucleare (INFN); allocations of computer time by the Computer Centre of Pavia University and CILEA (Consorzio Interuniversitario Lombardo per l' Elaborazione Automatica, Segrate – Milan), as well as by CINECA (Centro Interuniversitario Nord–Est di Calcolo Automatico, Casalecchio di Reno - Bologna), are gratefully acknowledged. H. Chamati's stay at Pavia University was made possible by a NATO–CNR fellowship; financial support as well as scientific hospitality are gratefully acknowledged; the authors also thank Prof. V. A. Zagrebnov (CPT–CNRS and Université de la Méditerranée, Luminy, Marseille, France) for helpful discussions.

* Present and permanent address: Institute of Solid State Physics, 72 Tzarigradsko Chaussée, 1784 Sofia, Bulgaria.
† Corresponding author.Electronic address: Silvano.Romano@pv.infn.it

1 P. Minnhagen, Rev. Mod. Phys. **59**, 1001 (1987).
2 Z. Gulácsi and M. Gulácsi , Adv. Phys. **47**, 1 (1998).
3 D.R. Nelson, Defects and Geometry in Condensed Matter Physics, University Press, (Cambridge, 2002)
4 Ya. G. Sinaĭ, *Theory of Phase Transitions; Rigorous Results*, (Pergamon Press, Oxford, 1982).
5 H.-O. Georgii, *Gibbs Measures and Phase Transitions*, (de Gruyter, Berlin-New York, 1988).
6 J. Fröhlich and T. Spencer, Commun. Math. Phys. **81**, 527 (1981).
7 R. Gupta, J. De Lapp, G. G. Batrouni, G. C. Fox, C. F. Baillie, and J. Apostolakis, Phys. Rev. Lett. **61**, 1996 (1988)
8 M. Hasenbusch, J. Phys. A **38**, 5869 (2005).
9 J. Tobochnik and G.V. Chester, Phys. Rev. B **20** 3761 (1979),
10 F. Dunlop, J. Stat. Phys. **41**, 733 (1985).
11 A. Cuccoli, V. Tognetti, P. Verrucchi, and R. Vaia, J. Appl. Phys. **76**, 6362 (1994).
12 A. Cuccoli, V. Tognetti, and R. Vaia, Phys. Rev. B **52**, 10221 (1995).
13 H. G. Evertz and D. P. Landau, Phys. Rev. **B 54**, 12302 (1996).
14 C. Gruber, H. Tamura and V. Zagrebnov, J. Stat. Phys. **106** (2002) 875.
15 S. Romano, Int. J. Mod. Phys. B **13**, 191 (1999).
16 S. Romano and R. O. Sokolovskii, Phys. Rev. B **61**, 11379 (2000).
17 J. L. Cardy and D. J. Scalapino, Phys. Rev. B **19**, 1428 (1979).
18 A. N. Berker and D. R. Nelson, J. Appl.Phys. **50**, 1799 (1979).
19 A. N. Berker and D. R. Nelson, Phys. Rev. B **19**, 2488 (1979).
20 Yu. E. Lozovik, and L. M. Pomirchy, Solid State Commun. **89**, 145 (1994).
21 L. M. Castro, A. S. T. Pires, and J. A. Plascak, J. Magn. Magn. Mater. **248**, 62 (2002).
22 S. A. Leonel, P. Z. Coura, A. R. Pereira, L. A. S. Mól, and B. V. Costa, Phys. Rev. B 67, 104426 (2003).
23 B. Berche, A. I. Fariñas-Sánchez, Yu. Holovatch, and R. Paredes V, Eur. Phys. J. B 36, 91 (2003).
24 T. Surungan and Y. Okabe, Phys. Rev. B **71**, 184438 (2005).
25 G.M. Wysin, A.R. Pereira, I.M. Marques, S.A. Leonel and P.Z. Coura, Phys. Rev. B **72**, 94418 (2005).
26 S. Romano, and V. A. Zagrebnov, Phys. Lett. A **301**, 402 (2002).
27 H. Chamati, S. Romano, L. A. S. Mól, and A. R. Pereira. Europhys. Lett. **72**, 62 (2005).
28 H. Chamati and S. Romano, Phys. Rev. B **71**, 64424 (2005)
29 M. P. Allen and D. J. Tildesley, *Computer Simulation of Liquids*, Oxford University Press, (Oxford, UK, 1989).
30 H. Chamati and S. Romano, Phys. Rev. B **71**, 64444 (2005)
31 S. Romano, Int. J. Mod. Phys. B **9**, 85 (1995).
32 R. Hashim and S. Romano, Int. J. Mod. Phys. B **13**, 3879 (1999).
33 S. T. Bramwell and P. C. W. Holdsworth, J. Phys. Condens. Matter **5**, L53 (1993).
34 S. T. Bramwell and P. C. W. Holdsworth, Phys. Rev. B **49**, 8811 (1994).